

New Design for an Integrated Fourier Transform Spectrometer

Omar Manzardo^{*}, Hans Peter Herzig, Benedikt Guldemann, Cornel Marxer, Nico de Rooij

Institute of Microtechnology, University of Neuchâtel, Breguet 2, 2000 Neuchâtel, Switzerland

ABSTRACT

We present a miniaturized Fourier transform (FT) spectrometer based on silicon micromachining. The FTS is a Michelson interferometer with one scanning mirror. The motion of the mirror is carried out by an electrostatic comb drive actuator. The mirror displacement is 39 μm and its reproducibility is ± 13 nm, which leads to a resolution better than 10 nm in the visible wavelength range. A new design of this chip has been realized in order to integrate an input fiber, a collimating lens system as well as a beam splitting plate. This new design allows to undertake spectroscopy with white light. The limitations of light collimation and the effect of the size of the source have been studied by numerical simulations.

Keywords: Fourier spectroscopy, actuator, MOEMS

1. INTRODUCTION

Fourier transform spectroscopy is a well-known technique to measure the spectra of weak extended sources. It offers throughput and multiplex advantages, which provide higher signal-to-noise ratio performance than other methods¹. However, commonly used FT spectrometers require a mirror scanning mechanism with very high precision, resulting in large size and high cost. Low cost, miniature spectrometers are key components, which enable the realization of small size, portable sensor solutions for applications, such as color measurements, or industrial process control. Therefore, recent investigations deal with low cost, miniature spectrometers. A spatially modulated FT spectrometer (e.g. a Michelson interferometer with a tilted mirror and a photodiode array) leads to compactness and has no moving parts. Nevertheless, stationary FT spectrometers have poor resolution and do not benefit entirely from the throughput advantage. We report here on a FT spectrometer with a moving mirror which is extremely compact (5 mm x 5 mm) and which has a scanning system that allows a precise motion of the mirror. It permits low cost fabrication thanks to silicon technology.

In Fourier transform spectroscopy, we measure the intensity variation I_R as a function of the optical path difference δ when a partially coherent plane wave is introduced into a Michelson interferometer. The relation between I_R and δ is known as an interferogram. The power spectrum $B(\sigma)$ and the recorded intensity modulation $I_R(\delta)$ are related by a Fourier transform:

$$B(\sigma) = \int_{-\infty}^{\infty} I_R(\delta) \exp(-i2\pi\sigma\delta) d\delta, \quad (1)$$

where σ is the wavenumber ($\sigma = 1/\lambda$). The theoretical resolution of a FT spectrometer is given by

$$\Delta\sigma = 1/\delta_{\max}, \quad (2)$$

where $\delta_{\max} = 2\Delta x_{\max}$ and Δx_{\max} is the maximum displacement of the mirror.

^{*} Correspondance: Email: omar.manzardo@imt.unine.ch; Web: <http://www-optics.unine.ch/>; Telephone: +41 32 718 3361; Fax: +41 32 718 3201

2. SPECTROMETER SET-UP

Recently, we have presented an actuator driving the mirror in a Michelson interferometer². The motion of the mirror is carried out by an electrostatic comb drive actuator. The mirror displacement is 39 μm and its reproducibility is ± 13 nm, which leads to a spectral resolution better than 10 nm in the visible wavelength range.

The actuator used to drive the movable mirror in our FT spectrometer enables a linear voltage-displacement response. In order to realize a linear motion of the mirror we have placed two identical comb drive actuators opposite to each other, named A and B (Fig. 3). When the voltage on comb A is kept constant and is exactly the opposite of V_B , i.e. $V_A = -V_B$, then the displacement Δx is

$$\Delta x = \frac{1}{k} \varepsilon_0 n \frac{h}{g} 2V_A V_0 \quad (3)$$

where k is the spring constant of the suspension springs, h is the height of the comb fingers, g the gap between the comb fingers, n is the number of comb fingers on the mobile comb and ε_0 is the electric permittivity. The applied voltage V_0 is modulated linearly from +10 V to -10 V, which leads to an optical path difference maximum δ_{max} of 77 μm .

We have observed a drive non-linearity $\Delta\delta(\delta)$ of up to ± 1 μm , as well as an hysteresis effect (Fig. 1).

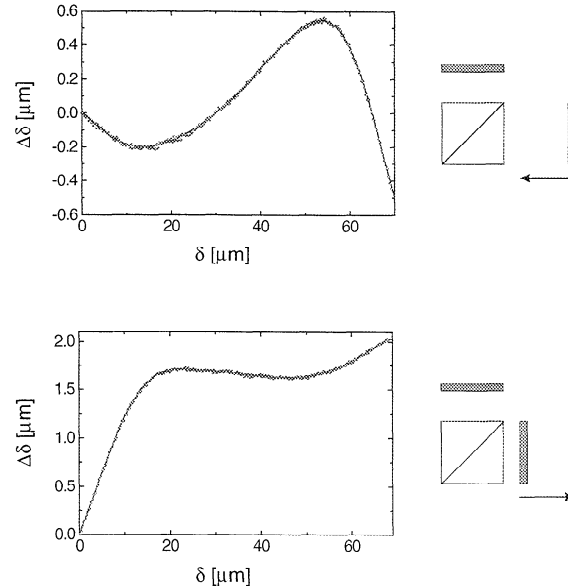


Fig. 1. Non-linearity $\Delta\delta(\delta)$ of the mobile mirror: results of the interferometric measurements for both directions of the motion.

This effect comes mainly from the change of the capacitance between the two combs when the displacement Δx becomes large. To get rid of the drive non-linearity, a phase correction is effectuated. Consequently the Fourier transform is corrected by taking into account the interferometric measurements of $\Delta\delta(\delta)$:

$$B(\sigma) = \int_{-\infty}^{\infty} I_R(\delta) \exp[-i2\pi\sigma(\delta + \Delta\delta(\delta))] d\delta \quad (3)$$

Figure 2 shows the spectrum of a HeNe laser before and after the phase correction. After the correction, the resolution is 6nm (at 633 nm) which is close to the theoretical limit. The correction applied to one scan is applied to other scans in the

same scan direction resulting in a resolution always better than 10 nm. The reproducibility of the mirror position, given as the optical path difference, is ± 25 nm.

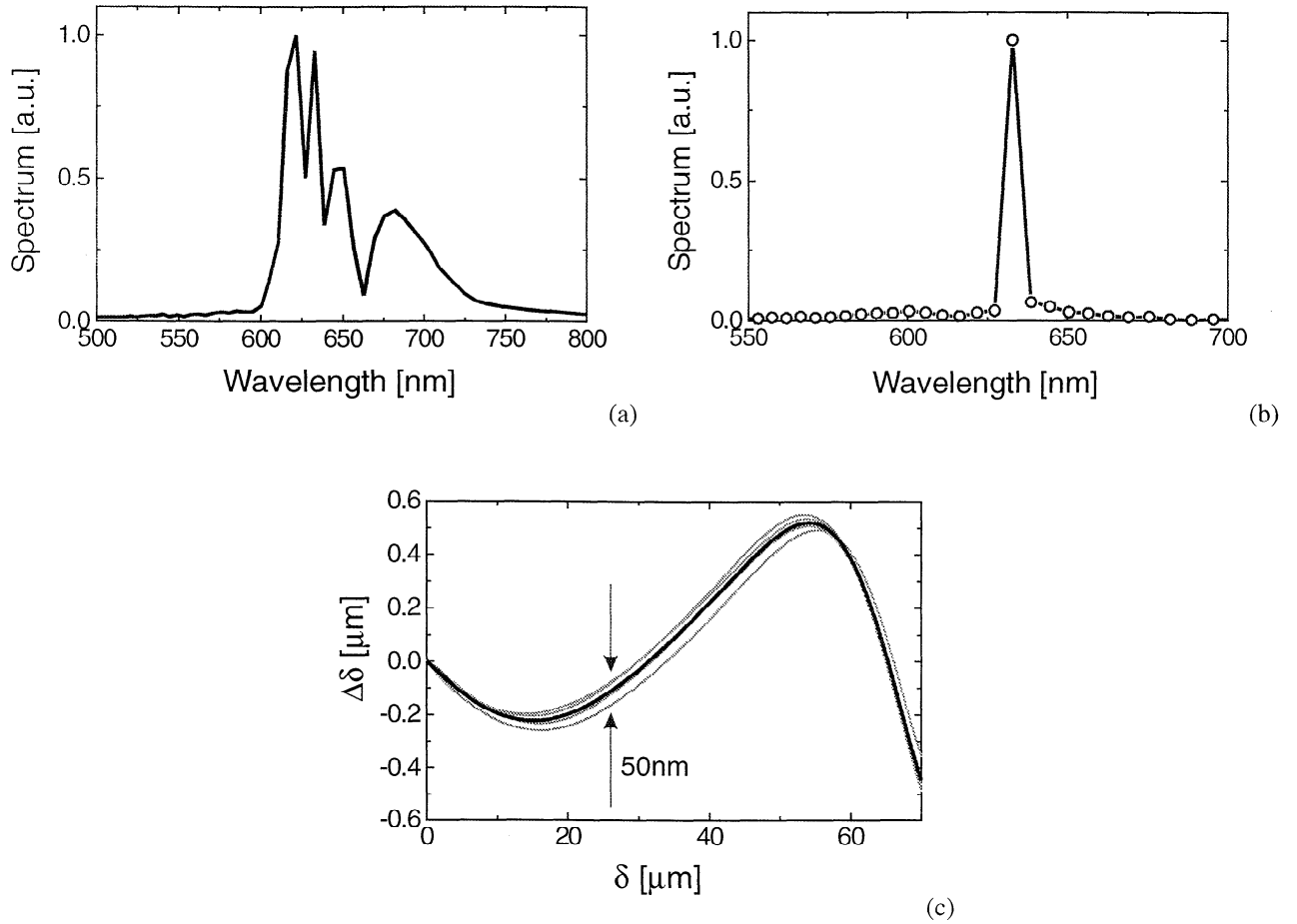


Fig. 2. Spectrum of a HeNe laser ($V_0 = \pm 10$ V and $\delta_{\text{max}} = 77 \mu\text{m}$) (a) before and (b) after the phase correction. (c) Deviance of the non-linearity $\Delta\delta(\delta)$ for several scans in the same direction. The reproducibility of the path length is better than ± 25 nm.

A new design has been developed in order to undertake measurements with light having small coherence length. Figure 3 shows a drawing of the chip configuration and Fig. 4 shows a SEM picture of the chip.

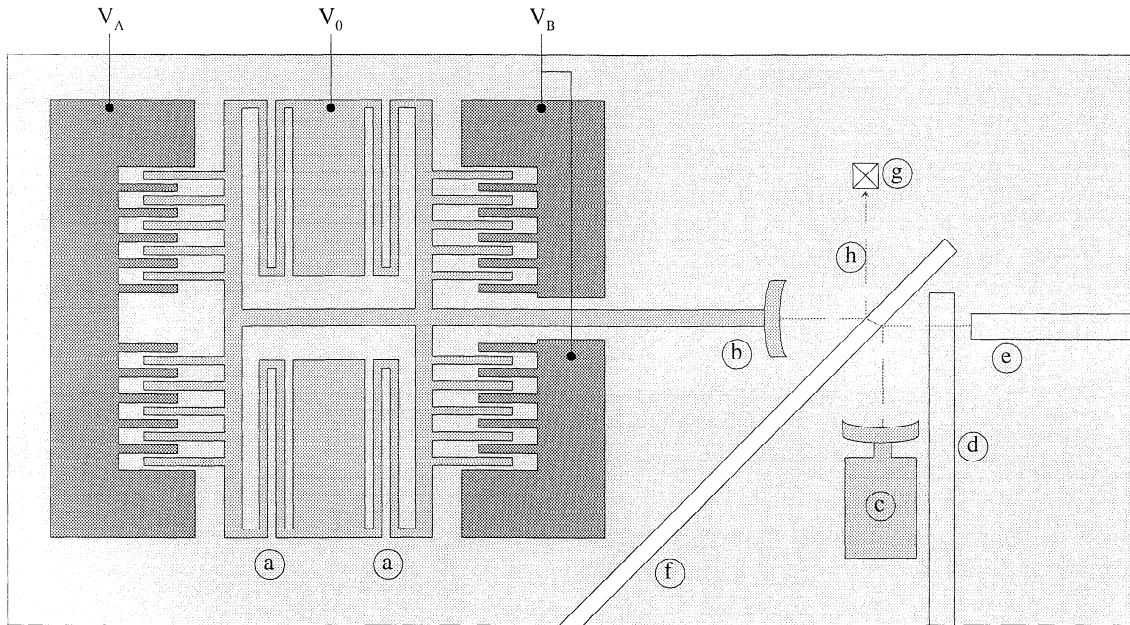


Fig. 3. Drawing of the new design with its important features: (a) springs; (b) movable mirror; (c) fixed mirror; (d) collimating fiber; (e) input fiber; (f) slit through the wafer for accommodation of the beam splitting plate; (g) single pixel detector; (h) optical beam. Voltage V_A and V_B are kept constant and V_0 varies linearly from +10 V to -10 V.

We propose two different designs. In the first one, emphasis is put on the collimation quality of the light, while in the second design we privilege assembly easiness and reduction of the optical distance from the input fiber to the detector. Special attention has been paid to set the optical path zero, that is the position where the two beams have a phase difference of zero. For obvious reasons, the alignment of the optical components is a crucial point and is ensured by a dedicated structuring of the chip.

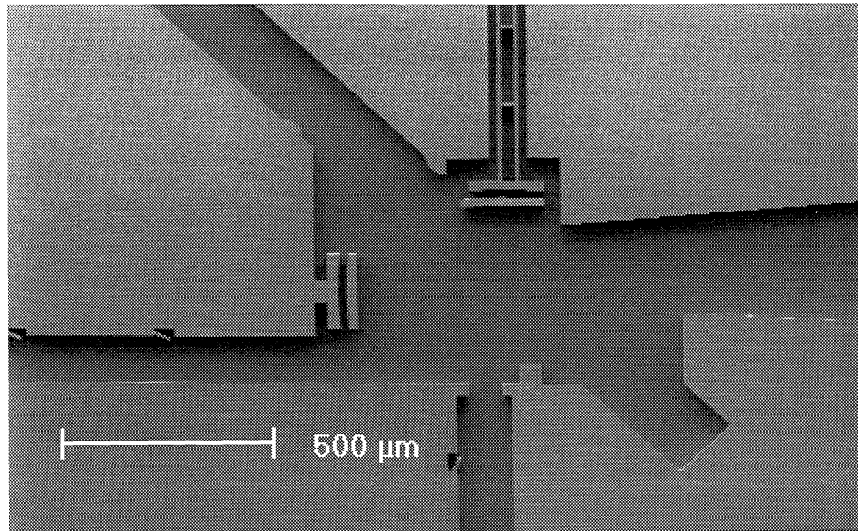


Fig. 4. SEM picture of the chip used for Fourier transform spectroscopy.

In the first design, collimation is ensured by crossed cylindrical elements: a gradient-index cylindrical micro-lens (fiber) and a cylindrical mirror. The collimating fiber (feature (d) in Fig. 3) is placed at a distance of 31 μm from the input fiber and

collimates the light diverging vertically to the surface of the chip. The two mirrors (features (b) and (c) in Fig. 3) have both a curvature that collimates the light diverging horizontally with the chip. Their size is $200\ \mu\text{m} \times 75\ \mu\text{m}$. The input fiber and the collimating fiber are fixed in U-grooves. The beam splitting plate is positioned by mean of a slit through the wafer.

In the second design, the light source is not collimated. The use of an external collimating system like a gradient-index cylindrical micro-lens (fiber) is avoided as well as the cylindrical mirrors. The optical distance from the input fiber to the detector is reduced from $700\ \mu\text{m}$ to $450\ \mu\text{m}$. This allows to collect all the light coming from the fiber ($\text{NA} = 0.2$).

In the first design, the light is well collimated, therefore the interference pattern is insensitive to the lateral position of the detector, because the interference is always issued from two quasi-plane waves. Unfortunately the distance from the source to mirrors is too long. The input fiber has a numerical aperture of 0.2, which corresponds, for a mirror of $200\ \mu\text{m}$, at a distance from the source to the mirrors of $500\ \mu\text{m}$ and this leads to a waste of light. In addition to that, a continuous curvature of the mirrors is difficult to obtain, because the selectivity of silicon is extremely high. The curved surfaces are obtained by a succession of segments. These facets appear in the mask used for the photolithography.

In the second design, the only external feature is the beam splitting plate. By avoiding any collimating element, the distance from the source to the mirrors is ideal for collecting all the light of the source. The limitation arising from the non-continuous curvature of the mirrors disappears.

The detection of the modulation is carried out by a single pixel detector, which is not yet integrated in the chip.

The plate can be fabricated by replication into UV-curing adhesive by mean of elastomeric material³ and the splitting surface is obtained by evaporation of silver. Elastomeric material is used to realize a negative mold of the original optical element and UV-curing is used to make the replicated copy. Figures 5 and 6 show different kind of structures in silicon designed to be optical components like cylindrical lenses or beam splitting plates.

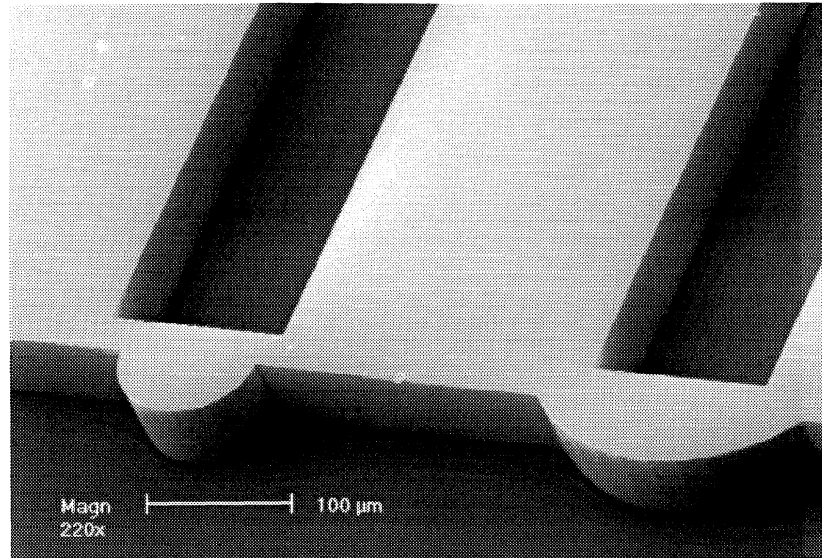


Fig. 5. Silicon structures (here, cylindrical lenses with U-grooves for input fiber) used for replication in UV glue.

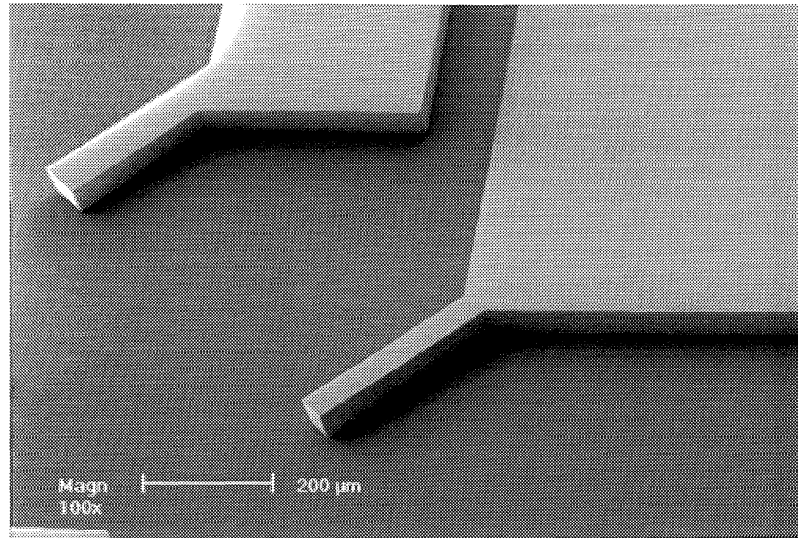


Fig. 6. Beam splitting plates and U-grooves in silicon ready for replication.

The advantage of such replicated optical elements is the precision of the alignment. It becomes therefore possible to design an optical bench, which can be fixed on the silicon chip by means of dedicated alignment marks in order to obtain a compact, self-aligned and easy-to-set system combining micro-optics and micro-mechanics.

3. COLLIMATION AND EXTENDED SOURCE

The collimation of the light source (e.g. an input fiber) is an important point. In such optical micro-systems, a trade-off between optical quality of the beam, compactness and performance has to be found. Conventional Fourier transform spectrometers operate in the infra-red range. They provide high resolution and need therefore macroscopic optical elements. The movable mirrors, for example, have sometimes driving distances of a few meters. Consequently the beam needs to be perfectly collimated. In our application, a resolution of a few nanometers in the visible range is enough. Therefore, it is possible to consider a bad collimated or even non-collimated beam.

A second element to be considered, is the spatial coherence, i.e. the influence of the size of the source on the interference pattern in function of the optical path difference. Figure 7 shows the important parameters to be taken into account in such a system.

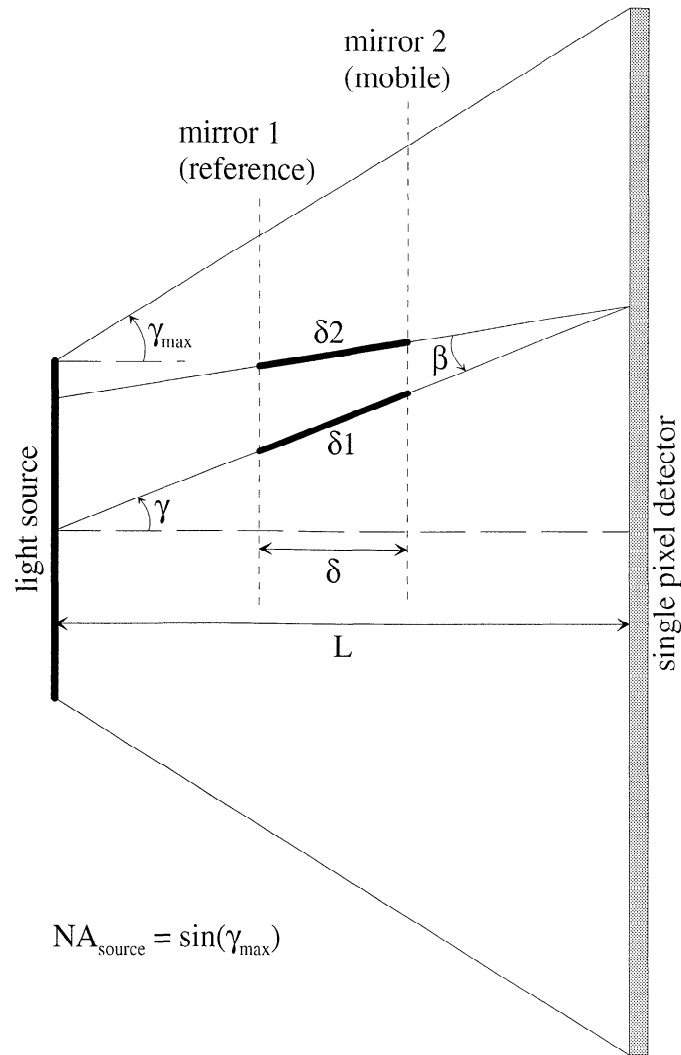


Fig. 7. Drawing showing the important parameters which influence collimation and spatial coherence. The set-up parameters are given by the extension of the light source, the position δ between the two mirrors (the reference mirror and the mobile mirror) and the distance from the source to the detector. The interference pattern and therefore the quality of the detection in function of δ is determined by the angles γ and β . In this drawing, $\delta = 2\Delta x$, where Δx is the real displacement of the mirror.

In a non-collimated configuration, the effective optical path difference (δ_i in Fig. 7) created by the mirror displacement Δx varies in function of the divergence angle γ . Figure 8 shows how δ_i varies in function of γ and gives the resulting interference pattern generated by a non-collimated point source with a numerical aperture $NA = 0.2$. It has to be noted that in such an example, the phase delay generated by $\delta_i(\gamma)$ is about 2λ when γ is equal to the numerical aperture of the source. This value is higher than conventional phase differences allowed in other systems, e.g. spatially modulated interferometers (e.g. a Michelson-based FT spectrometer with a tilted mirror) where a phase difference of more than $\lambda/4$ is harmful. Despite this fact, it is shown in Fig. 10 that a modulation in function of δ can still be detected. It has then to be pointed out that this configuration is tolerant against phase distortion due to a poor collimation.

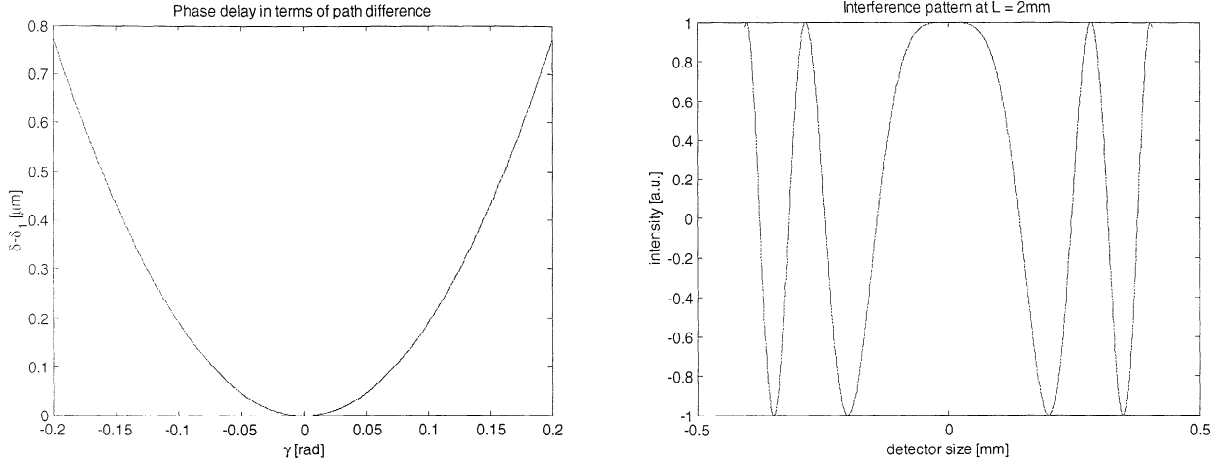


Fig. 8. Left: effective optical difference δ_i in function of the divergence angle γ . Right: simulated interference pattern generated by a non-collimated point source. In this example, the NA of the source is 0.2, the wavelength is 380 nm and the distance from the source to the detector is 2 mm.

The description of the extended source and the generated interference pattern in function of the optical path difference δ is a 1D model. The extension of the source has been simulated by a line of point sources emitting rays having a Lambert distribution of the intensities in function of the divergence angle γ :

$$I(\gamma) = I_0 \cos\left(\frac{2\pi\gamma}{\sin^{-1}(NA)}\right) \quad (4)$$

The point sources are mutually incoherent. Consequently, the intensity modulation generated by the single sources is summated. Figure 9 shows three interference patterns generated by a source with a size of 50 μm. The figure shows the evolution of the interference pattern at three different δ . The detector integrates the entire pattern and therefore the contrast decreases while δ increases (see Fig. 9). From the same figure we can determine the size of the detector necessary to detect the entire pattern in order to collect all the light.

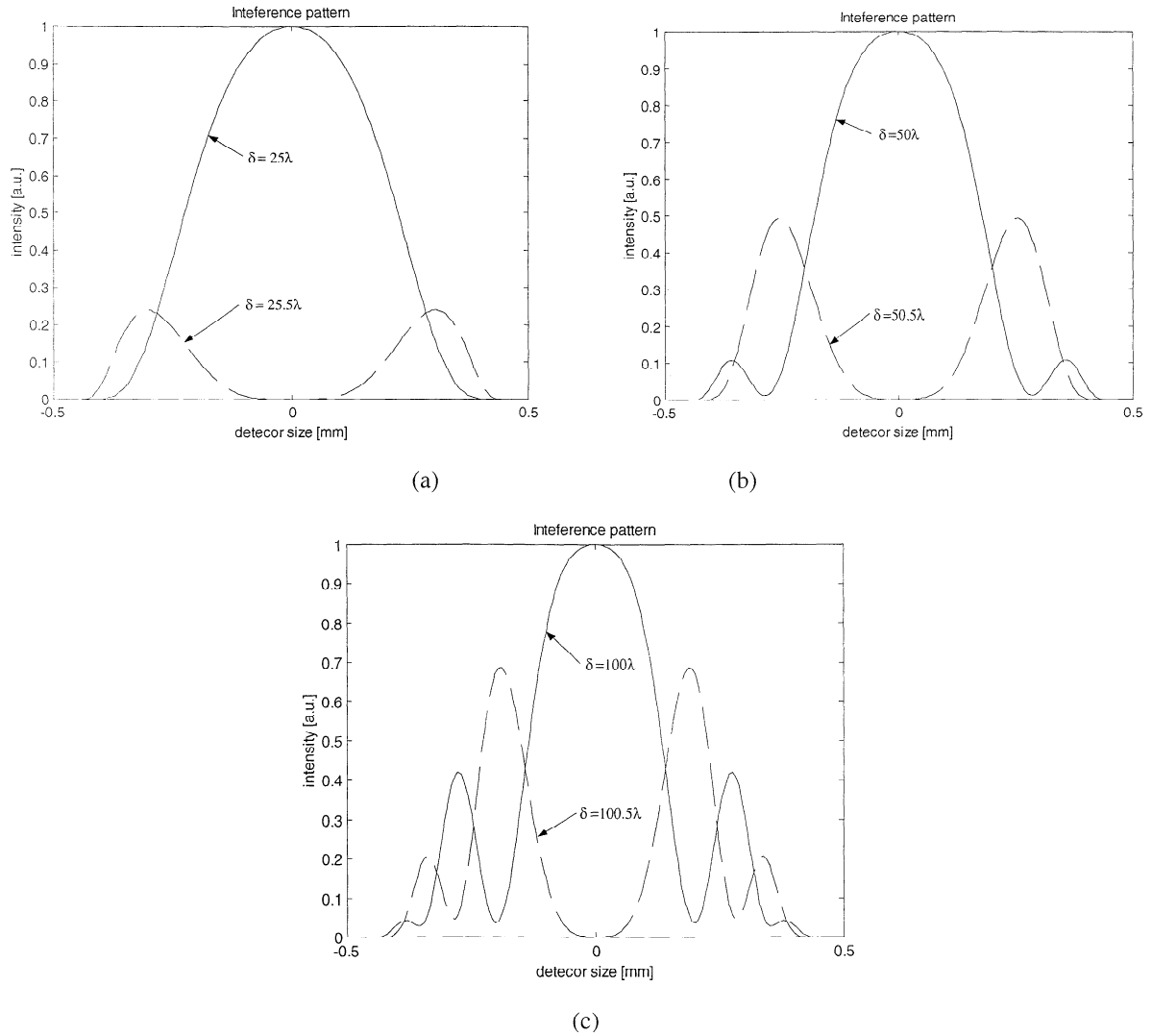


Fig. 9. Interference patterns generated by a source of $50 \mu\text{m}$. The NA of the source is 0.2, the wavelength is 380 nm and the distance from the source to the detector is 2 mm . Solid lines represent constructive interference patterns (i.e. δ is a multiple of the wavelength) and dashed lines represent destructive interference patterns (i.e. $\delta \propto \lambda + \lambda/2$). (a) $\delta \approx 9.5 \mu\text{m}$; (b) $\delta \approx 19 \mu\text{m}$; (c) $\delta \approx 38 \mu\text{m}$.

It can be illustrated by Fig. 9 that, even with large optical path differences δ , the difference (in terms of detected power) between a constructive and a destructive interference is still significant. This means that a modulation of the detected power in function of δ can still be detected. The decrease of contrast, because of the degradation of the optical quality of the interference pattern in function of δ , is illustrated in Fig. 10.

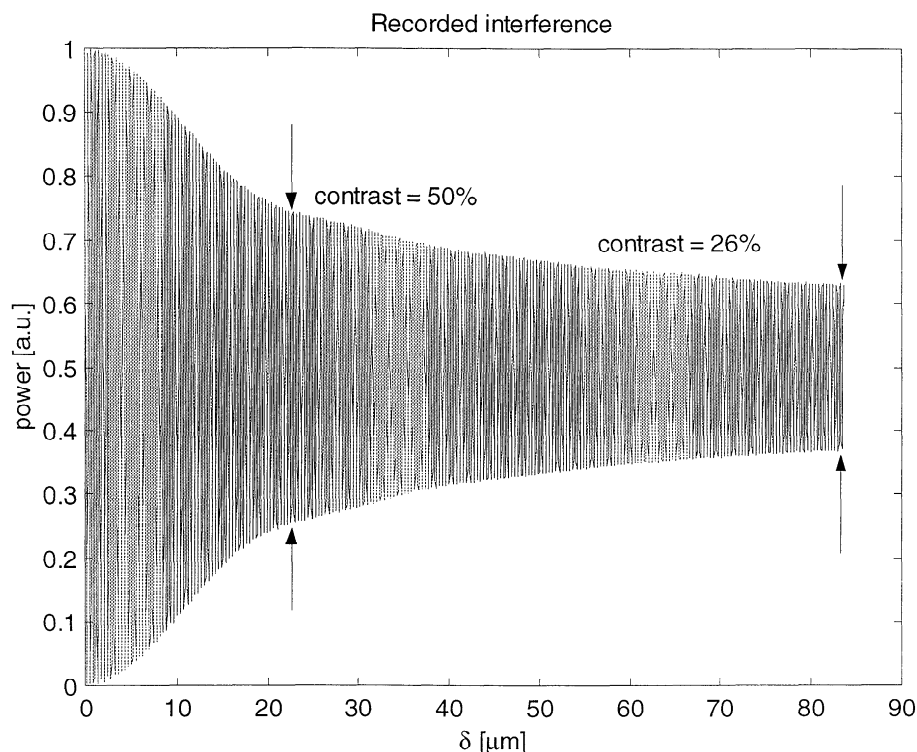


Fig. 10. Simulated modulation of the interference pattern generated by a source of 50 μm in function of the optical path difference δ . The NA of the source is 0.2, the wavelength is 380 nm and the distance from the source to the detector is 2 mm. The contrast is 50% after an optical path difference of 22 μm . At $\delta_{\text{max}} = 80$ μm , the modulation is still detectable but the contrast is 26%.

4. CONCLUSIONS

A low cost miniaturized (5 mm x 5 mm) time-scanning FTS, with a moving mirror activated by a new electrostatic actuator design has been realized. The feasibility of the device has been demonstrated by preliminary measurements with a HeNe laser. From the recorded interferograms it appears that the movable mirror has a drive non-linearity of about 1.3 %. The phase correction gives a spectrum of the HeNe line with a resolution of 6 nm. The same correction has been applied to other scans yielding a resolution better than 10 nm. The repeatability of the motion of the mirror is better than ± 13 nm. The resolution is good enough for applications such as industrial color sensors. The chip concept enables a high accuracy of the position of the optical path zero. The chip contains a collimating system which does not demand an external adjustment. With a collimated beam, the optical path maximum can, in theory, be infinite. Simulations have been carried out in order to study the limits of a configuration without collimating system, which leads to a simplified set-up. The results show that the modulation of the detected power, in function of the optical path difference δ , is still detectable for δ equal to the maximum path difference that can be obtained with this actuator.

5. REFERENCES

1. R.J Bell, "Introductory Fourier Transform Spectroscopy", Academic Press, New York, 1972.
2. O. Manzardo, H. P. Herzig, C. R. Marxer, N. F. de Rooij, "Miniaturized time-scanning Fourier transform spectrometer based on silicon technology", Opt. Lett. **24**, 1705 (1999).
3. P. Nussbaum, I. Philipoussis, A. Husser, H. P. Herzig, "Simple technique for replication of micro-optical elements", Opt. Eng. **36**(6), 1804 (1998).